2

Wavelet Transformations

2.1 INTRODUCTION

Wavelet transformations play a central role in the study of self-similar signals and systems. As we will see, the wavelet transform constitutes as natural a tool for the manipulation of self-similar or scale-invariant signals as the Fourier transform does for translation-invariant signals such as stationary, cyclostationary, and periodic signals. Furthermore, just as the discovery of fast Fourier transform (FFT) algorithms dramatically increased the viability of Fourier-based processing of translation-invariant signals in real systems, the existence of fast discrete wavelet transform (DWT) algorithms for implementing wavelet transformations means that wavelet-based representations for self-similar signals are also of great practical significance.

In terms of history, the theory of wavelet transformations dates back to the work of Grossmann and Morlet [5], and was motivated by applications in seismic data analysis [6]. This inspired much subsequent work by several individuals over the next several years on a general mathematical theory. For example, several key results in the theory of nonorthogonal wavelet expansions are described by Daubechies [7] [8]. In this book, however, we are primarily interested in *orthonormal* wavelet bases. The development of such bases, and their interpretation in the context of multiresolution signal analysis, is generally attributed to Meyer [9] and Mallat [10] [11]. However, it was Daubechies who introduced the first highly practical families of orthonormal wavelet bases in her landmark paper [12].

Yet although wavelet theory is rather new, it is important to note at the outset that many of the ideas underlying wavelets are not new. Indeed, wavelet theory can be viewed as a convenient and useful mathematical framework for formalizing and relating some well-established methodologies from a number of diverse areas within mathematics, physics, and engineering. Examples include:

- pyramidal image decompositions in computer vision [13],
- multigrid methods in the solution of partial-differential and integral equations [14],
- spectrogram methods in speech recognition [15],
- progressive transmission algorithms and embedded coding in communications [16] [17] [18], and
- multirate filtering algorithms in digital audio [19] [20], speech and image coding [21] [22], voice scrambling [23], frequency division data multiplexing [24], and time/frequency division data cross-multiplexing [20].

In fact, wavelet transformations are closely associated with a number of topics that have been extensively explored in the signal processing literature in particular, including constant-Q filter banks and time-frequency analysis [25], and quadrature mirror, conjugate quadrature, and other related multirate filter banks [20]. Vetterli and Kovačević [22], for example, explore such connections in detail.

This chapter is designed as a self-contained overview of wavelet transformations in general and of orthonormal wavelet transformations in particular. Its primary purpose is to establish some notational conventions for wavelets and to summarize the key results from wavelet theory we exploit in the applications in subsequent chapters. In introducing the theory of wavelet transformations, we adopt a rather tutorial style and emphasize a strongly signal processing perspective. While a number of excellent introductions to wavelet theory can be found in the literature (see, e.g., [7] [11] [26] [27]) we stress that the one presented here emphasizes a perspective that is particularly important in light of the applications that are the focus of this book.

2.2 WAVELET BASES

Most generally, the wavelet transformation of a signal $x(t)$

$$x(t) \longleftrightarrow X_\nu^\mu$$

is defined in terms of projections of $x(t)$ onto a family of functions that are all normalized dilations and translations of a prototype "wavelet" function

$\psi(t)$, i.e.,

$$\mathcal{W}\{x(t)\} = X_\nu^\mu = \int_{-\infty}^{\infty} x(t)\,\psi_\nu^\mu(t)\,dt \tag{2.1}$$

where

$$\psi_\nu^\mu(t) = |\mu|^{-1/2}\,\psi\left(\frac{t-\nu}{\mu}\right).$$

In this notation, μ and ν are the continuous dilation and translation parameters, respectively, and take values in the range $-\infty < \mu, \nu < \infty$, $\mu \neq 0$. A necessary and sufficient condition for this transformation to be invertible is that $\psi(t)$ satisfy the *admissibility condition*

$$\int_{-\infty}^{\infty} |\Psi(\omega)|^2\,|\omega|^{-1}\,d\omega = C_\psi < \infty, \tag{2.2}$$

where $\Psi(\omega)$ is the wavelet's Fourier transform, defined as [1]

$$\Psi(\omega) = \int_{-\infty}^{\infty} \psi(t)\,e^{-j\omega t}\,dt.$$

Provided $\psi(t)$ has reasonable decay at infinity and smoothness, as is usually the case in practice, (2.2) is equivalent to the admissibility condition

$$\int_{-\infty}^{\infty} \psi(t)\,dt = 0. \tag{2.3}$$

For any admissible $\psi(t)$, the synthesis formula corresponding to the analysis formula (2.1) is then

$$x(t) = \mathcal{W}^{-1}\{X_\nu^\mu\} = \frac{1}{C_\psi}\int_{-\infty}^{\infty}\int_{-\infty}^{\infty} X_\nu^\mu\,\psi_\nu^\mu(t)\,\mu^{-2}\,d\mu\,d\nu. \tag{2.4}$$

Under certain circumstances, it is also possible to reconstruct $x(t)$ solely from samples of X_ν^μ on a hyperbolic lattice defined by

$$\begin{aligned} \mu &= a^{-m} \\ \nu &= n\,b\,a^{-m} \end{aligned}$$

where $-\infty < m < \infty$ and $-\infty < n < \infty$ are the integer dilation and translation indices, respectively, and a and b are the corresponding dilation and translation increments. In such cases, the corresponding countably infinite collection of functions $\psi_\nu^\mu(t)$ is said to constitute a **frame**. A general theory and some iterative reconstruction algorithms are presented by Daubechies [7] [8]. However, it is also possible to construct wavelets and lattices such that the resulting transformation is not only invertible, but *orthonormal* as well. In general, orthonormal transformations are extremely convenient analytically, and possess very nice numerical properties. Consequently, it is this class of wavelet transformations that is of primary interest in this work, and the theory is summarized in the sequel.

2.3 ORTHONORMAL WAVELET BASES

Our focus in this section is on the particular case of ***dyadic*** **orthonormal wavelet bases**, corresponding to the case $a = 2$ and $b = 1$ for which the theory is comparatively more fully developed. In Section 2.3.7, however, we construct a simple family of orthonormal wavelet bases corresponding to lattices defined by $a = (L+1)/L$ and $b = L$ where $L \geq 1$ is an integer.

An orthonormal wavelet transformation of a signal $x(t)$

$$x(t) \longleftrightarrow x_n^m$$

can be described in terms of the synthesis/analysis equations[1]

$$x(t) = \mathcal{W}_d^{-1}\{x_n^m\} = \sum_m \sum_n x_n^m\,\psi_n^m(t) \tag{2.5a}$$

$$x_n^m = \mathcal{W}_d\{x(t)\} = \int_{-\infty}^{\infty} x(t)\,\psi_n^m(t)\,dt \tag{2.5b}$$

and has the special **property** that the orthogonal basis functions are all dilations and translations of a single function referred to as the *basic wavelet* (or "**mother**" **wavelet**) $\psi(t)$. In particular,

$$\psi_n^m(t) = 2^{m/2}\,\psi(2^m t - n) \tag{2.6}$$

where m and n are the dilation and translation indices, respectively.

An important example of a wavelet basis, and one to which we refer on numerous occasions throughout the book, is that derived from the ideal bandpass wavelet, which we specifically denote by $\tilde{\psi}(t)$. This wavelet is the impulse response of an ideal bandpass filter with frequency response

$$\tilde{\Psi}(\omega) = \begin{cases} 1 & \pi < |\omega| \leq 2\pi \\ 0 & \text{otherwise} \end{cases}. \tag{2.7}$$

It is straightforward to verify that the dilations and translations of $\tilde{\psi}(t)$ constitute an orthonormal basis for the vector space[2] of finite-energy signals $L^2(\mathbb{R})$. However, there are many other examples of orthonormal wavelet bases.

The basic wavelet $\psi(t)$ typically has a Fourier transform $\Psi(\omega)$ that satisfies several more general properties. First, because for a fixed m the $\{\psi_n^m(t)\}$

[1] For notational brevity, summations are over all integers, i.e., unless otherwise specified,

$$\sum_n = \sum_{n=-\infty}^{\infty}.$$

[2] A detailed treatment of the notation, concepts, and geometry of vector spaces that provides a background for this chapter can be found in, for example, Naylor and Sell [28] or Reed and Simon [29].

constitute an orthonormal set we get the Poisson formula

$$\sum_k |\Psi(\omega - 2\pi k)|^2 = 1$$

and, in turn, the bound

$$|\Psi(\omega)| \leq 1. \tag{2.8a}$$

Moreover, from (2.3) we have immediately

$$\Psi(0) = 0. \tag{2.8b}$$

Finally, we are generally interested in *regular* bases, i.e., bases comprised of regular basis functions. Regularity is a measure of the smoothness of a function. In particular, a function $f(t)$ is said to be Rth-order regular if its Fourier transform $F(\omega)$ decays according to[3]

$$F(\omega) \sim \mathcal{O}\left(|\omega|^{-R}\right), \qquad |\omega| \to \infty.$$

We use the term "regular" to denote a function that is at least first-order regular, and note that an Rth-order regular function has $R-1$ regular derivatives. Consequently, in order for our wavelet basis to be regular we require that

$$\Psi(\omega) \sim \mathcal{O}\left(|\omega|^{-1}\right), \qquad |\omega| \to \infty. \tag{2.8c}$$

As implied by (2.8a)–(2.8c), $\psi(t)$ is often the impulse response of an at least roughly bandpass filter. Consequently, the wavelet transformation can usually be interpreted either in terms of a generalized constant-Q (specifically, octave-band) filter bank, or, as we will see later, in terms of a multiresolution signal analysis. While we restrict our attention to this class of wavelet bases, it is important to remark, however, that wavelets need not correspond to either an octave-band filter bank or a multiresolution analysis. For example, the following wavelet due to Mallat [30]

$$\Psi(\omega) = \begin{cases} 1 & \text{if} \quad 4\pi/7 < |\omega| \leq \pi \quad \text{or} \quad 4\pi < |\omega| \leq 32\pi/7 \\ 0 & \text{otherwise} \end{cases}$$

generates a perfectly valid orthonormal wavelet basis, but does not correspond to a multiresolution analysis.

[3]The order notation $\mathcal{O}(\cdot)$ has the following interpretation: if

$$F(\omega) = \mathcal{O}(G(\omega)), \qquad \omega \to \infty$$

then

$$\lim_{\omega \to \infty} \frac{F(\omega)}{G(\omega)} < \infty.$$

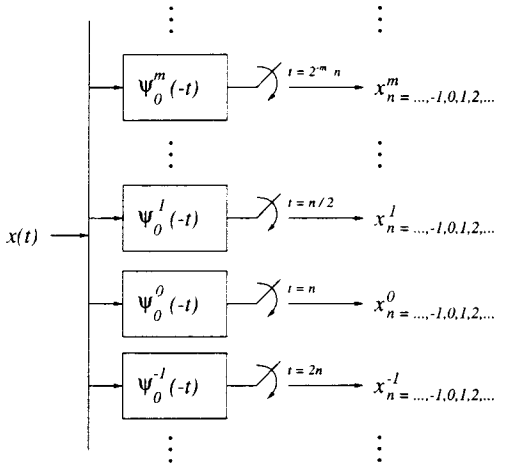

Figure 2.1. Critically sampled filter bank interpretation of an orthonormal wavelet decomposition.

2.3.1 An Octave-Band Filter Bank Interpretation

The filter bank interpretation of the wavelet transform arises by viewing the analysis equation (2.5b) as a *filter-and-sample* operation, viz.,

$$x_n^m = \{x(t) * \psi_0^m(-t)\}|_{t=2^{-m}n}.$$

Although the interpretation applies more generally, it is often convenient to visualize the basis associated with the ideal bandpass wavelet (2.7). In this case, the output of each filter in the bank is sampled at the corresponding Nyquist rate. More generally, we say that the filter bank is *critically sampled* [25], in that reconstruction is not possible if any of the sampling rates are reduced regardless of the choice of wavelet. The critically sampled filter bank corresponding to the wavelet decomposition is depicted in Fig. 2.1.

For a particular choice of wavelet basis, the magnitude of the frequency response of the filters in such a filter bank is portrayed in Fig. 2.2. As this figure illustrates, there can be significant spectral overlap in the magnitude responses while preserving the orthogonality of the decomposition. In essence, while the frequency response magnitudes are not supported on disjoint frequency intervals, perfect reconstruction and orthogonality are achieved due to the characteristics of the phase in the filters, which leads to cancellation of aliasing effects in the reconstruction. However, it is important to emphasize that it is possible to construct wavelet bases such that the spectral overlap between channels is much smaller in applications where this is important.

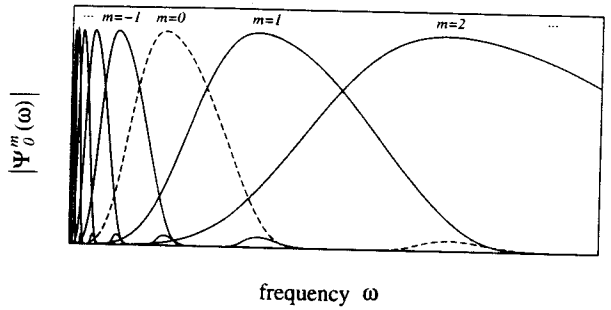

Figure 2.2. The octave band filters corresponding to an orthonormal wavelet decomposition. The wavelet basis in this example is one due to Daubechies [12].

A filter bank decomposition is closely related to the notion of a local time-frequency analysis. Provided the filters are reasonably bandpass in character, the output of each filter in the bank is an estimate of the frequency content in the signal localized to the corresponding frequency band. Likewise, provided the filter impulse responses are localized in time, the sequence of output samples from each filter gives a picture of the time-evolution of frequency content within the corresponding frequency band. In the case of the **wavelet decomposition**, $(x_n^m)^2$ represents an estimate of the energy of the signal $x(t)$ in the vicinity of $t \approx 2^{-m}n$, and for a band of frequencies in the neighborhood of $\omega \approx 2^m\pi$. This is graphically depicted in the time-frequency plane of Fig. 2.3(a). Note that the octave-band frequency partitioning leads to a partitioning of the time axis that is finer in the higher (and wider) frequency bands. We emphasize that the partitioning in this figure is idealized: in accordance with the Fourier transform uncertainty principle, one cannot have perfect localization in both time and frequency. Nevertheless, one can construct wavelet bases whose basis functions have their energy concentrated at least roughly according to this partitioning.

In contrast to the wavelet transform, the familiar short-time Fourier transform representation of a signal corresponds to a filter bank in which the filters are modulated versions of one another and, hence, have equal bandwidth. As a consequence, the outputs are sampled at identical rates, and the corresponding time-frequency analysis is one in which there is uniform partitioning of both the time and frequency axes in the time-frequency plane, as depicted in Fig. 2.3(b).

While the wavelet transform analysis equation (2.5b) can be interpreted in terms of a filter bank decomposition, the corresponding *synthesis* equation (2.5a) may be interpreted, as depicted in Fig. 2.4, as multirate modulation

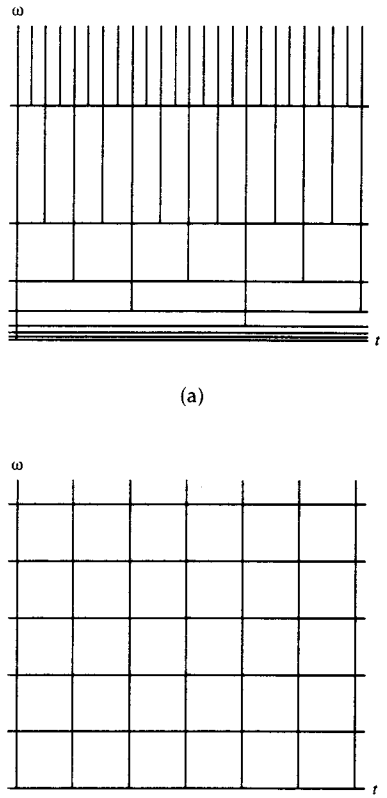

Figure 2.3. Time-frequency portraits corresponding to two signal analyses. (a) Wavelet transformation. (b) Short-time Fourier transformation.

in which for a given m each sequence of coefficients x_n^m is modulated onto the corresponding wavelet dilate $\psi_0^m(t)$ at rate 2^m. For the case of the ideal bandpass wavelet, this corresponds to modulating each such sequence x_n^m into the distinct octave frequency band $2^m\pi < \omega \leq 2^{m+1}\pi$.

The filter bank interpretation allows us to readily derive the following useful identity

$$\sum_m |\Psi(2^{-m}\omega)|^2 = 1 \tag{2.9}$$

valid for all orthonormal wavelet bases and any $\omega \neq 0$. To see this, consider an arbitrary finite-energy signal $x(t)$ with Fourier transform $X(\omega)$, which is decomposed into an orthonormal wavelet basis via the filter bank of Fig. 2.1,

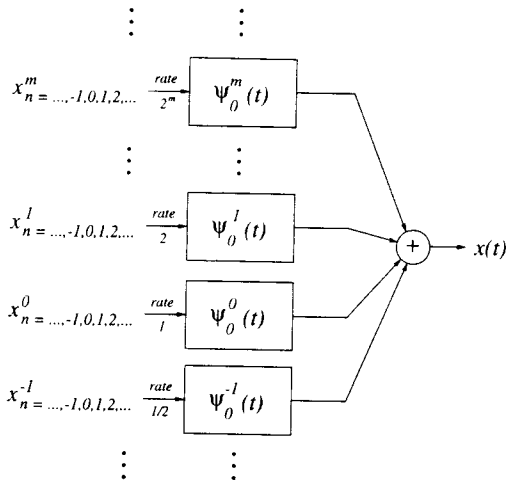

Figure 2.4. Interpretation of an orthonormal wavelet expansion as a multirate modulation scheme.

then immediately re-synthesized according to the filter bank of Fig. 2.4. It is a straightforward application of sampling theory to show that the Fourier transform of the output of this cascade can be expressed as

$$X(\omega)\sum_m |\Psi(2^{-m}\omega)|^2 + \sum_{k\neq 0}\sum_m X(\omega - 2\pi k\, 2^m)\Psi(2^{-m}\omega)\Psi^*(2^{-m}\omega - 2\pi k).$$

Since this must be equal to $X(\omega)$, the terms on the right must all be zero, while the factor multiplying $X(\omega)$ must be unity, yielding the identity (2.9) as desired.

While the filter bank interpretation provides a natural, convenient, and familiar framework in which to view orthonormal wavelet transformations, it is also possible to view the transformation in the context of a multiresolution signal analysis framework [9] [11] [12]. This perspective, which we consider next, provides a number of rich new insights into orthonormal wavelet bases.

2.3.2 Multiresolution Signal Analysis Interpretation

In general, a multiresolution signal analysis is a framework for analyzing signals based on isolating variations in the signal that occur on different temporal or spatial scales. This strategy underlies a variety of diverse signal processing algorithms including pyramidal methods used in the solution of computer vision problems [31] and multigrid methods used in the solution of

boundary value problems [14]. The basic analysis algorithm involves approximating the signal at successively coarser scales through repeated application of a smoothing or averaging operator. At each stage, a differencing operation is used to extract a detail signal capturing the information *between* consecutive approximations. The matching synthesis algorithm involves a successive refinement procedure in which, starting from some coarsest scale approximation, detail signals are accumulated in order to generate successively finer scale signal approximations.

Orthonormal wavelet bases can be interpreted in the context of a particular class of linear multiresolution signal analyses in which signal approximations at all resolutions of the form 2^m (for m an integer) are defined. In describing this class, we begin formally by restricting our attention to the vector space of finite-energy signals $\mathbf{V} = L^2(\mathbb{R})$. A multiresolution signal analysis is then defined as a decomposition of this signal space $\mathbf{V}$ into a sequence of subspaces

$$\ldots, \mathbf{V}_{-1}, \mathbf{V}_0, \mathbf{V}_1, \mathbf{V}_2, \ldots$$

such that each $\mathbf{V}_m$ contains signal approximations at a resolution 2^m. Associated with each $\mathbf{V}_m$ is a linear operator $A_m\{\cdot\}$ that defines projections from anywhere in $\mathbf{V}$ onto $\mathbf{V}_m$. That is, for each signal $x(t) \in \mathbf{V}$, the projection $A_m\{x(t)\} \in \mathbf{V}_m$ defines the closest signal of resolution 2^m to $x(t)$,

$$A_m\{x(t)\} = \arg\min_{v(t)\in\mathbf{V}_m} \|x(t) - v(t)\|.$$

Central to the concept of multiresolution signal analysis is the notion of being able to construct successively coarser resolution approximations by repeated application of a smoothing operator. Mathematically, this characteristic is obtained by imposing the nesting or causality relation

$$\mathbf{V}_m \subset \mathbf{V}_{m+1}, \tag{2.10a}$$

which specifically ensures that the approximation of a signal at resolution 2^{m+1} contains all the information necessary to approximate the signal at the coarser resolution 2^m, i.e.,

$$A_m\{A_{m+1}\{x(t)\}\} = A_m\{x(t)\}.$$

The relations

$$\overline{\bigcup_{m=-\infty}^{\infty} \mathbf{V}_m} = \mathbf{V} \tag{2.10b}$$

$$\bigcap_{m=-\infty}^{\infty} \mathbf{V}_m = \{0\} \tag{2.10c}$$

ensure that a complete range of approximations is defined by the analysis. In the process, these completeness relations define arbitrarily good and arbitrarily poor approximations that are consistent with any intuitive notion of

resolution, i.e.,

$$\lim_{m\to\infty} A_m\{x(t)\} = x(t)$$
$$\lim_{m\to-\infty} A_m\{x(t)\} = 0.$$

An additional relation is required to fully define the notion of resolution: signals in $\mathbf{V}_m$ must be characterized by 2^m samples per unit length. Mathematically, this can be interpreted as requiring that there exist a one-to-one correspondence or "isometry" between each subspace of signals $\mathbf{V}_m$ and the vector space of finite-energy sequences $\mathbf{I} = \ell^2(\mathbb{Z})$

$$\mathbf{V}_m \overset{\text{isom}}{\longleftrightarrow} \mathbf{I} \tag{2.10d}$$

such that each sequence represents samples of the corresponding signal following some potentially rather arbitrary linear processing:

$$x(t) \in \mathbf{V}_m \;\Rightarrow\; \varphi_m\{x(t)\}|_{t=2^{-m}n} \in \mathbf{I} \tag{2.10e}$$

where $\varphi_m\{\cdot\}$ is a linear operator.

In general, eqs. (2.10a)–(2.10e) are adequate to define a multiresolution signal analysis. However, imposing two additional constraints leads to an analysis with some convenient structure. The first is a translation-invariance constraint, viz.,

$$x(t) \in \mathbf{V}_m \;\Leftrightarrow\; x(t - 2^{-m}n) \in \mathbf{V}_m \tag{2.10f}$$

which ensures that the nature of the approximation of the signal $x(t)$ is the same for any time interval. It is this condition that leads to the translational relationships among basis functions in the corresponding wavelet expansion. The second is a scale-invariance constraint

$$x(t) \in \mathbf{V}_m \;\Leftrightarrow\; x(2t) \in \mathbf{V}_{m+1} \tag{2.10g}$$

which ensures that the nature of the approximation at each resolution is the same. In turn, it is this condition that gives rise to the dilational relationships among basis functions in the corresponding wavelet expansion.

It can be shown [30] that every such multiresolution analysis, i.e., every collection of subspaces $\mathbf{V}_m$ defined in accordance with (2.10a)–(2.10g), is completely characterized in terms of a *scaling function* (or "father" wavelet) $\phi(t)$. Consequently, from the scaling function one can construct an orthonormal basis for each $\mathbf{V}_m$, and, hence, the approximation operator $A_m\{\cdot\}$ for each of these subspaces. In particular, for each m,

$$\ldots, \phi_{-1}^m(t), \phi_0^m(t), \phi_1^m(t), \phi_2^m(t), \ldots$$

constitutes an orthonormal basis for $\mathbf{V}_m$, where the basis functions, as a consequence of the invariance constraints (2.10f) and (2.10g) imposed on the multiresolution analysis, are all dilations and translations of one another, i.e.,

$$\phi_n^m(t) = 2^{m/2}\phi(2^m t - n). \tag{2.11}$$

The corresponding resolution-2^m approximation of a signal $x(t)$ is then obtained as the projection of $x(t)$ onto $\mathbf{V}_m$, which, exploiting the convenience of an orthonormal basis expansion, is expressed as

$$A_m\{x(t)\} = \sum_n a_n^m \phi_n^m(t) \tag{2.12}$$

with the coefficients a_n^m computed according to the individual projections

$$a_n^m = \int_{-\infty}^{\infty} x(t)\,\phi_n^m(t)\,dt. \tag{2.13}$$

In general, $\phi(t)$ has a Fourier transform $\Phi(\omega)$ that is at least roughly lowpass. Using an argument similar to that which led to (2.8a), orthonormality of the basis $\{\phi_n^m(t)\}$ implies that

$$|\Phi(\omega)| \le 1. \tag{2.14a}$$

Additionally, because this basis for $\mathbf{V}_m$ is asymptotically complete in $\mathbf{V}$ [cf. (2.10b)] we have

$$|\Phi(0)| = 1. \tag{2.14b}$$

Finally, since we are, again, generally interested in *regular* bases, we must have

$$\Phi(\omega) \sim \mathcal{O}\left(|\omega|^{-1}\right), \qquad \omega \to \infty. \tag{2.14c}$$

Collectively, the properties (2.14a)–(2.14c) describe a scaling function that is consistent with the notion that $A_m\{\cdot\}$ is an approximation or smoothing operator. Consequently, we may interpret the projection (2.13) as a lowpass-like filter-and-sample operation, viz.,

$$a_n^m = \{x(t) * \phi_0^m(-t)\}|_{t=2^{-m}n}. \tag{2.15}$$

Moreover, (2.12) can be interpreted as a modulation of these samples onto a lowpass-like waveform.

In fact, one example of a multiresolution analysis is generated from the ideal lowpass scaling function $\tilde{\phi}(t)$, whose Fourier transform is the frequence response of an ideal lowpass filter, i.e.,

$$\tilde{\Phi}(\omega) = \begin{cases} 1 & |\omega| \le \pi \\ 0 & |\omega| > \pi \end{cases}. \tag{2.16}$$

In this case, the corresponding multiresolution analysis is based upon perfectly bandlimited signal approximations. Specifically, for a signal $x(t)$, $\tilde{A}_m\{x(t)\}$ represents $x(t)$ bandlimited to $\omega = 2^m\pi$. Furthermore, we may interpret (2.15) and (2.12) in the context of classical sampling theory [32]. In particular, $\tilde{\phi}(t)$ in (2.15) plays the role of an anti-aliasing filter [3], while (2.12) is the interpolation formula associated with the sampling theorem.

Of course, there are practical difficulties associated with the implementation of a multiresolution analysis based upon perfectly bandlimited approximations, foremost of which is that the sampling and reconstruction filters,

i.e., the $\phi_0^m(t)$, are unrealizable. For this reason, this analysis is primarily of interest for its conceptual rather than practical value.

To derive the wavelet basis associated with each multiresolution analysis defined via (2.10), we now shift our attention from the sequence of increasingly coarse scale *approximation* signals $A_m\{x(t)\}$ to the *detail* signals representing the information lost at each stage as the resolution is halved. The collection of resolution-limited signal approximations constitutes a highly redundant representation of the signal. By contrast, the collection of detail signals constitutes a much more efficient representation. Formally, we proceed by decomposing each space $\mathbf{V}_{m+1}$ into the subspace $\mathbf{V}_m$ and its orthogonal complement subspace $\mathbf{O}_m$, i.e., $\mathbf{O}_m$ satisfies

$$\mathbf{O}_m \perp \mathbf{V}_m \tag{2.17a}$$

$$\mathbf{O}_m \oplus \mathbf{V}_m = \mathbf{V}_{m+1}, \tag{2.17b}$$

where we recognize that it is in this orthogonal complement subspace that the detail signal resides.

Associated with every multiresolution analysis is a basic wavelet $\psi(t)$ which yields the following orthonormal basis for each $\mathbf{O}_m$

$$\ldots, \psi_{-1}^m(t), \psi_0^m(t), \psi_1^m(t), \psi_2^m(t), \ldots$$

where $\psi_n^m(t)$ is as defined in terms of dilations and translations of $\psi(t)$ as per (2.6). In turn, this leads to a convenient description of the projection operator $D_m\{\cdot\}$ from anywhere in $\mathbf{V}$ onto $\mathbf{O}_m$ as

$$D_m\{x(t)\} = \sum_n x_n^m \psi_n^m(t)$$

in terms of the individual projections [cf. (2.5b)]

$$x_n^m = \int_{-\infty}^{\infty} x(t)\, \psi_n^m(t)\, dt.$$

Hence, we have the interpretation that the wavelet coefficients x_n^m for a fixed m correspond to the detail signal $D_m\{x(t)\}$ at scale 2^m, or, more specifically, to the information in the signal $x(t)$ between the resolution-2^m and resolution-2^{m+1} approximations, i.e.,

$$D_m\{x(t)\} = A_{m+1}\{x(t)\} - A_m\{x(t)\}.$$

At this point, we recognize the wavelet associated with the bandlimited multiresolution analysis defined via (2.16) to be the ideal bandpass wavelet (2.7); it suffices to consider a frequency domain perspective. To complete the discussion, we observe that via (2.17) we can recursively decompose any of the approximation subspaces $\mathbf{V}_M$, for some M, into the direct sum of a sequence of orthogonal subspaces, i.e.,

$$\mathbf{V}_M = \mathbf{O}_{M-1} \oplus \mathbf{V}_{M-1} = \mathbf{O}_{M-1} \oplus (\mathbf{O}_{M-2} \oplus \mathbf{V}_{M-2}) = \cdots = \bigoplus_{m<M} \mathbf{O}_m. \tag{2.18}$$

from which we see that for every $x(t)$

$$A_M\{x(t)\} = \sum_{m<M} D_m\{x(t)\} = \sum_{m<M} \sum_n x_n^m \psi_n^m(t). \tag{2.19}$$

This leads naturally to the interpretation of $A_M\{x(t)\}$ as an approximation in which details on scales smaller than 2^M are discarded. Letting $M \to \infty$ in (2.19) yields

$$x(t) = \sum_m \sum_n x_n^m \psi_n^m(t),$$

the synthesis formula (2.5a), and corresponds to the subspace decomposition

$$\mathbf{V} = \bigoplus_{m=-\infty}^{\infty} \mathbf{O}_m.$$

Our interpretation of an orthonormal wavelet basis as a multiresolution signal analysis is then complete.

2.3.3 Discrete Wavelet Transform

The discrete wavelet transform (DWT) refers to a discrete-time framework for implementing the orthonormal wavelet transform. The basic notion is that rather than implementing the analysis directly as a sequence of continuous-time filter-and-sample operations according to (2.3.1), the analysis can be reformulated into a single continuous-to-discrete conversion procedure followed by some iterative discrete-time processing. Likewise, the synthesis can be reformulated from a series of conventional modulations (2.5a) into an iterative discrete-time procedure followed by a single discrete-to-continuous conversion.

The implementation is based upon the discrete-time filters

$$h[n] = \int_{-\infty}^{\infty} \phi_n^1(t)\, \phi_0^0(t)\, dt \tag{2.20a}$$

$$g[n] = \int_{-\infty}^{\infty} \phi_n^1(t)\, \psi_0^0(t)\, dt. \tag{2.20b}$$

Typically, $h[n]$ and $g[n]$ have discrete-time Fourier transforms [3]

$$H(\omega) = \sum_n h[n]\, e^{-j\omega n}$$

$$G(\omega) = \sum_n g[n]\, e^{-j\omega n}$$

that have roughly halfband lowpass and highpass characteristics, respectively. In fact, for the particular case of bandlimited multiresolution signal analysis, the corresponding filters, which we distinguish using the notation

$\tilde{h}[n]$ and $\tilde{g}[n]$, are *ideal* lowpass and highpass filters; specifically

$$\tilde{H}(\omega) = \begin{cases} 1 & 0 < |\omega| \le \pi/2 \\ 0 & \pi/2 < |\omega| \le \pi \end{cases}$$
$$\tilde{G}(\omega) = \begin{cases} 0 & 0 < |\omega| \le \pi/2 \\ 1 & \pi/2 < |\omega| \le \pi \end{cases}.$$

More generally, as we will see, the filters $h[n]$ and $g[n]$ form a conjugate quadrature filter pair.

The analysis algorithm is structured as follows. Given a signal $x(t) \in \mathbf{V}$ from which we would like to extract x_n^m for $m < M$, we can obtain the approximation coefficients a_n^{M+1} via the filter-and-sample procedure of (2.15), then recursively apply the following filter-downsample algorithm

$$a_n^m = \sum_l h[l-2n]\, a_l^{m+1} \tag{2.21a}$$
$$x_n^m = \sum_l g[l-2n]\, a_l^{m+1} \tag{2.21b}$$

to extract the transform coefficients x_n^m corresponding to successively coarser scales m. A detailed derivation of this algorithm is presented in Appendix A.

The synthesis algorithm is structured in a complementary fashion. In particular, to reconstruct $x(t)$ to resolution 2^{M+1} from x_n^m for $m \le M$, we can recursively apply the upsample-filter-merge algorithm

$$a_n^{m+1} = \sum_l \{h[n-2l]\, a_l^m + g[n-2l]\, x_l^m\} \tag{2.21c}$$

to compute the coefficients a_n^m of successively finer scale approximations until level $m = M$ is reached, after which $A_{M+1}\{x(t)\}$ may be constructed by modulating a_n^M according to (2.12). A detailed derivation of this algorithm is also left to Appendix A.

Fig. 2.5 depicts the discrete-time relationships between approximation and detail coefficients corresponding to adjacent scales. The complete algorithm for computing wavelet coefficients based on the discrete wavelet transform is depicted in Fig. 2.6.

The DWT may be computed extremely efficiently using polyphase forms. Indeed, if the filters $h[n]$ and $g[n]$ have length L, an implementation of the DWT via an FFT-based algorithm generally has an asymptotic computational complexity of $\mathcal{O}(\log L)$ per input sample [33]. However, as also discussed in [33] this figure can be somewhat misleading as there are many subtle issues associated with measuring complexity of the algorithm; a thorough treatment can be found in, e.g., Vetterli and Kovačević [22].

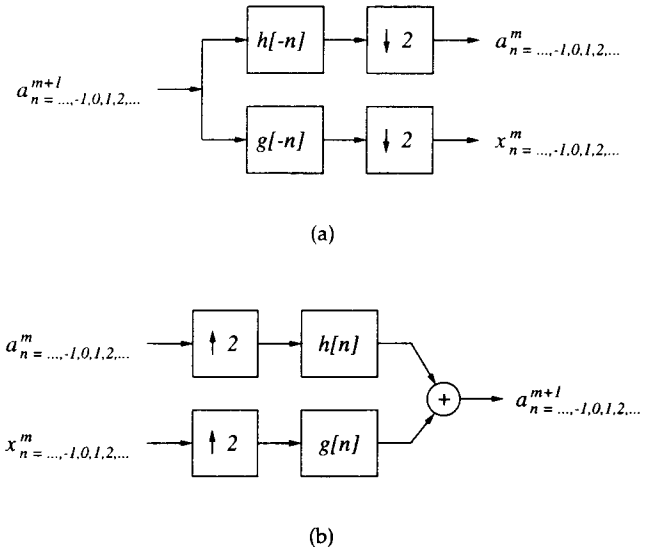

Figure 2.5. A single stage of discrete-wavelet transform algorithm. (a) The analysis step: filter-downsample. (b) The synthesis step: upsample-filter-merge.

2.3.4 Finite Data Length and Resolution Effects

In most applications, the data consists of a finite collection of samples

$$x[n], \qquad n = 0, 1, \ldots, N.$$

While it is usually assumed that the $x[n]$ correspond to samples of a *resolution-limited approximation* of a continuous-time signal $x(t)$, i.e.,

$$x[n] = a_n^{M+1} = \{\phi_n^{M+1}(-t) * x(t)\}\big|_{t=2^{-(M+1)}n}$$

for some M, this cannot always be justified. Nevertheless, if the signal $x(t)$ was processed by a typical anti-aliasing filter prior to sampling, then it is often a useful approximation, particularly if the anti-aliasing filter has characteristics similar to that of the smoothing filter $\phi_0^{M+1}(t)$ associated with the approximation operator.

Note that while the discrete-time nature of the data limits access to the finer scales of detail, the length of the observations limits access to the coarser scales of detail. Hence, in practice we typically have access to wavelet

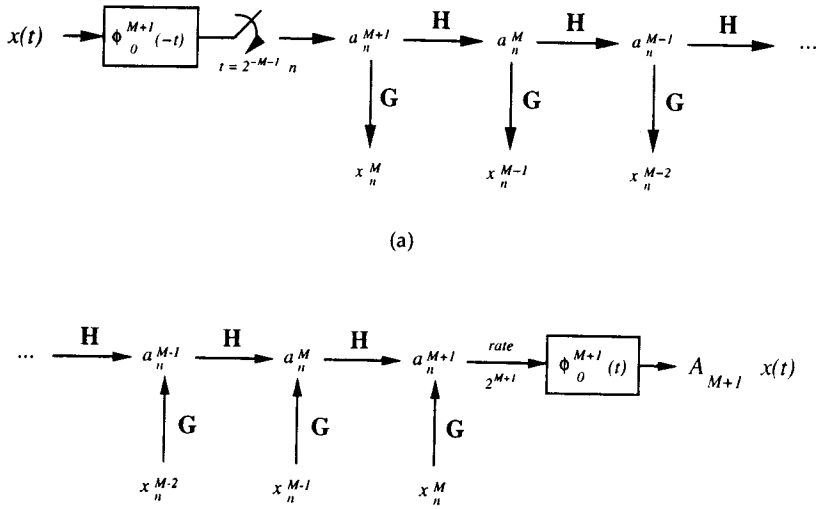

Figure 2.6. An efficient implementation of the orthonormal wavelet transformation based on the discrete wavelet transform. (a) The analysis algorithm. (b) The synthesis algorithm. The processing on each branch is as defined in Fig. 2.5.

coefficients over a finite range of scales for a given signal. Moreover, because the effective width of the wavelet basis functions halves at each finer scale, we expect roughly a doubling of the number of available coefficients at each successively finer scale. In a typical scenario, for a data record of $N = N_0 2^M$ samples, we would expect to be able to extract x_n^m corresponding to

$$\begin{aligned} m &= 1, 2, \ldots, M \\ n &= 0, 1, \ldots, N_0 2^{m-1} - 1 \end{aligned}$$

via the DWT, where N_0 is a constant that depends on the particular wavelet basis.

Note that while there are a number of ways to handle the unusual data windowing problem inherent in the wavelet decomposition, an assumption that the data is periodic outside the observation window leads to a computationally convenient implementation. This is the method we adopt in the simulations described in this book.

2.3.5 Orthonormal Wavelet Basis Constructions

As we have indicated, for every multiresolution analysis characterized by a scaling function, there exists an associated wavelet basis. In fact, it is possible to exploit the structure of the discrete wavelet transform to show how the wavelet $\psi(t)$ may always be derived directly from the scaling function $\phi(t)$. In this section we describe how this is accomplished. More generally, we show how one can construct a family of orthonormal wavelet bases directly from a class of discrete-time filters.

We begin by observing that there are a number of properties that the discrete-time filters $h[n]$ and $g[n]$ corresponding to a multiresolution signal must satisfy. For instance, as a consequence of the orthogonality constraints between the $\{\psi_n^m(t)\}$ and $\{\phi_n^m(t)\}$, one can show [30] that $h[n]$ and $g[n]$ must be related by

$$g[n] = (-1)^n h[1-n]$$

which, expressed in the frequency domain, is

$$G(\omega) = e^{-j\omega} H^*(\omega + \pi). \tag{2.22}$$

Furthermore, orthonormality of the $\{\phi_n^m(t)\}$ requires that $H(\omega)$ satisfy

$$|H(0)|^2 = 2 \tag{2.23a}$$

$$|H(\omega)|^2 + |H(\omega + \pi)|^2 = 2. \tag{2.23b}$$

Filter pairs that satisfy both (2.22) and (2.23) are termed conjugate quadrature filters (CQFs), and have been discussed extensively in the signal processing literature; see, e.g., Vaidyanathan [20].

We note that (2.22) leads immediately to an algorithm for constructing the wavelet corresponding to a particular scaling function: one can generate $h[n]$ from $\phi(t)$ via (2.20a), $g[n]$ from $h[n]$ via (2.22), then $\psi(t)$ from $g[n]$ and $\phi(t)$ via (A.1b). However, even more significantly, we note that $h[n]$ alone is also sufficient to fully characterize a wavelet basis through a multiresolution analysis. Indeed, given $h[n]$, the dilation equation[4] (A.1a) can be solved for the corresponding scaling function $\phi(t)$. In particular, $\phi(t)$ has Fourier transform

$$\Phi(\omega) = \prod_{m=1}^{\infty} \left[2^{-1/2} H(2^{-m}\omega)\right] \tag{2.24}$$

which is intuitively reasonable from a recursive decomposition of the corresponding frequency domain equation, viz., (A.2a).

In fact, the conditions (2.23) on $h[n]$ are necessary but not sufficient for (2.24) to generate a regular wavelet basis. However, choosing $h[n]$ to satisfy

[4] For a further discussion of dilation equations, see, e.g., Strang [26].

both (2.23) and to have a Fourier transform $H(\omega)$ with R zeros at $\omega = \pi$, i.e.,[5]

$$H^{(r)}(\pi) = 0, \qquad r = 0, 1, \ldots, R-1$$

is sufficient to generate a wavelet basis with Rth-order regularity. Moreover, in this case, we find, via (A.2a), that the wavelet has R vanishing moments:

$$\int_{-\infty}^{\infty} t^r \psi(t)\, dt = (j)^r \Psi^{(r)}(0) = 0, \qquad r = 0, 1, \ldots, R-1. \tag{2.25}$$

It is important to note, however, that the vanishing moment condition (2.25), while convenient and sufficient, is not necessary for regularity. For a more detailed discussion of necessary and sufficient conditions, see, e.g., Lawton [34].

A variety of useful wavelet bases have been constructed from CQF pair formulations of this type. In fact, this approach has been extremely useful in designing orthonormal wavelets with compact support, i.e., wavelets for which

$$\psi(t) = 0, \qquad |t| > T$$

for some $0 < T < \infty$. This is a consequence of the natural correspondence between compactly supported wavelets and the extensively developed theory of finite impulse response (FIR) digital filters. A more comprehensive development of the relationships between wavelet theory and filter bank theory can be found in, e.g., Vetterli and Kovačević [22].

2.3.6 Examples

In this section, we briefly review some standard examples of wavelet bases. Thus far, we have discussed only one example, the wavelet basis corresponding to the ideal bandpass wavelet (2.7). This basis has excellent frequency localization properties, but very poor time-domain localization. Indeed, the corresponding wavelet $\psi(t)$ decays only like $1/t$ for large t, and the CQF filters $h[n]$ and $g[n]$ decay only like $1/n$ for large n. More serious still, this basis is unrealizable.

At another extreme, consider a Haar-based multiresolution analysis in which the approximations at resolution 2^m are piecewise constant on intervals of length 2^{-m}. Here the scaling function is given by

$$\phi(t) = \begin{cases} 1 & 0 \le t < 1 \\ 0 & \text{otherwise} \end{cases}$$

and the corresponding wavelet is

$$\psi(t) = \begin{cases} 1 & 0 \le t < 1/2 \\ -1 & 1/2 \le t < 1 \\ 0 & \text{otherwise} \end{cases}.$$

[5] We use the notation $f^{(n)}(\cdot)$ for the nth derivative of a function $f(\cdot)$.

This analysis is realizable and exhibits excellent time localization but very poor frequency localization due to the abrupt time-domain transitions of the approximations. Indeed, $\Psi(\omega)$ falls off only like $1/\omega$ for $\omega \to \infty$.

Between these extremes lie a number of wavelet families. Consider, for example, the family of Battle-Lemarie wavelet bases [30] [12]. These bases may be derived from a multiresolution analysis based upon orthogonalized Pth-order spline functions. For these bases, the corresponding scaling function is given by

$$\Phi(\omega) = \frac{1}{\omega^{P+1}} \left[\sum_k \frac{1}{(\omega + 2\pi k)^{2(P+1)}} \right]^{-1/2}.$$

For example, the first-order ($P = 1$) Battle-Lemarie multiresolution analysis corresponds to piecewise-linear but continuous signal approximations. In this context, it is trivial to show that the Haar-based wavelet basis we have discussed corresponds to the case $P = 0$. Similarly, using a Central Limit Theorem argument it is possible to show that the bandpass wavelet basis corresponds to $P \to \infty$. In general, the Battle-Lemarie bases have very reasonable localization properties: they are characterized by exponential decay in the time domain and decay like $1/|\omega|^{P+1}$ in the frequency domain. Hence while they are, strictly-speaking, unrealizable, the exponential decay property ensures that good approximations may be realized via truncation.

As another family of examples, Daubechies has designed an important class of compactly supported wavelet bases [12] based upon discrete-time FIR filters. In addition to fulfilling a practical requirement of having finite-extent basis functions, these bases exhibit good localization in both time and frequency. The Rth-order Daubechies basis is characterized by CQF filters $h[n]$ and $g[n]$ of length $2R$ for $R = 1, 2, \ldots$, where the case $R = 1$ corresponds to the Haar-based wavelet basis. Moreover, the basis functions are *maximally regular*, in the sense that they have the maximum number of vanishing moments (R) for a given order.

In general, the development of other families of wavelet-based multiresolution analyses continues to receive considerable attention in the literature. For example, some with particularly attractive computational implementations are described in [35].

2.3.7 Nondyadic Orthonormal Wavelet Bases

While we have focused largely upon dyadic wavelet bases, for which the dilation and translation increments are $a = 2$ and $b = 1$, there are many other nondyadic choices. In many applications, including those within the context of this book, such generalizations are potentially very useful particularly for $1 < a < 2$. This is because these correspond to an analysis with finer

frequency resolution on the logarithmic frequency scale. For instance, it would be highly convenient to have the flexibility of choosing from among a family of bases corresponding to the lattice

$$\begin{aligned} a &= (L+1)/L \\ b &= L, \end{aligned}$$

where $L = 1, 2, \ldots$ is a parameter. An at least conceptually useful class of such bases arises out of a generalization of the ideal bandpass basis defined by

$$\Psi(\omega) = \begin{cases} \sqrt{L} & \pi < |\omega| \leq \dfrac{L+1}{L}\pi \\ 0 & \text{otherwise} \end{cases}$$

where the case $L = 1$ corresponds to the usual (dyadic) bandpass basis. It is a straightforward exercise in analysis to verify that for each L the corresponding set $\{\psi_n^m(t)\}$, for which

$$\psi_n^m(t) = \left(\frac{L+1}{L}\right)^{m/2} \psi\left(\left(\frac{L+1}{L}\right)^m t - nL\right),$$

is complete and orthonormal. Unfortunately, however, these basis functions have have tails that decay very slowly due to their ideal frequency characteristics. This leads to comparatively poor time-domain localization properties which considerably reduces the practical value of these particular bases. Constructions for more practical nondyadic wavelet basis have been pursued by, e.g., Auscher [36], Blu [37], and Kovačević and Vetterli [38].

2.4 SUMMARY

In this chapter, we presented those aspects of wavelet theory that will be important in the developments throughout the remainder of the book. Two interpretations of the orthonormal wavelet transform were discussed: one based on an octave-band filter bank framework; the other on a multiresolution signal analysis framework. Each provided rich and complementary insights into wavelet theory. Our treatment of the topic emphasized a signal processing perspective, and developed strong intuition in both the time and frequency domains.

The chapter also discussed several aspects of the implementation of the wavelet transform in practice, since these will be important when wavelets are exploited in the development of actual fractal signal processing algorithms in subsequent chapters. In particular, we discussed the discrete wavelet transform, a discrete-time algorithm for synthesizing and analyzing signals via the orthonormal wavelet transform. Related issues including the effects of finite data length and limited data resolution on the computation were

also discussed. The chapter concluded with several examples of families of wavelet bases that are important both conceptually and practically.